# Enhancement and Field Testing of a Dynamic Freeway Simulation Program

PANOS MICHALOPOULOS, EIL KWON, AND JEONG-GYU KANG

An enhanced version of KRONOS, a dynamic, microcomputer-based freeway simulation program, is presented. KRONOS is based on mesoscopic continuum modeling and explicitly treats the coupling effects of ramps on the freeway flow in detail. The major improvements of the new version include the substantial reduction of computer execution time and the addition of new simulation modules that can describe the flow behavior under restricted capacity situations, such as incidents and short-term construction. Further, a newly developed output interface links KRONOS with other advanced data management and analysis software, so that more detailed and flexible output analysis can be possible. In order to test and validate the program in real traffic environments, field data collection was performed at 26 locations covering an 8-mi section of the I-35W freeway in Minneapolis, Minnesota. The data consist of 5-min volume and speed information for each lane during three morning and three afternoon peak periods. The test results with the available data indicate satisfactory performance of the enhanced KRONOS program in light-to-moderate traffic conditions, although the error increased during heavy congestion.

A major problem in freeway operations and traffic management practice is to assess the effectiveness of changes or improvements before implementation. This process includes comparing alternative geometric configurations, estimating the effects of improvements, determining the adequacy of traffic management schemes, assessing the impacts of control strategies, studying the formation and dissipation of congestion on the freeway and its ramps, etc.

Although simulation methods have long been recognized as the most powerful tool for such analysis, most existing freeway simulation programs are still either in the development stage (*1*) or lack the sophistication necessary for applications requiring reasonably high performance levels (*1,2*). Furthermore, despite recent advances in microcomputer technologies, the most widely known simulation programs developed to date require mainframe computers (*3–6*) that are not readily available to most practicing engineers.

The major recent enhancements and field testing results of KRONOS (*7*), a microcomputer-based, dynamic freeway simulation program, which was developed during the mid-1980s to address these problems, are described. KRONOS is based on continuum flow modeling, which treats traffic as a compressible fluid. Unlike other macroscopic simulation programs, KRONOS explicitly models interrupted traffic flow behavior such as merging, lane changing, weaving, and diverging (*7–11*). The coupling effects of ramps on the main freeway are considered in determining the actual entering and exiting flows as well as in following the simultaneous development of queues and propagation of congestion on both the freeway and the ramps.

Although KRONOS has been almost continuously enhanced since the inception of its initial version (*7*), the most notable enhancements were made during the past 2 years. This includes substantial reduction of computer execution time by reorganizing the program structure using the C programming language. Further, the input/output (I/O) modules were extensively modified to take advantage of recent hardware advancements, such as single-screen systems with high-resolution graphics for both text and graphics displays. In addition, an output interface was developed to create spreadsheet-formatted output files, which enable the user to use more advanced data management and analysis software including Lotus 1–2–3. Consequently, much more flexible and detailed output analysis is now possible. Perhaps the most important enhancement lies in the modeling adjustments through improved determination of the boundary conditions as well as the extension of the program capacity to simulate virtually all types of freeway geometric conditions, which include merging and diverging of freeways, two-lane entrance and exit ramps, lane addition and deletion, left side ramps, etc. In order to validate the simulation model, an extensive field data collection was conducted from the selected locations covering an 8-mi section of the I-35W freeway in Minneapolis, Minnesota, for six peak periods in November 1989. The collected data, which consisted of 5-min volume and speed information of the freeway main line as well as of entrance and exit ramps, has been used for the validation of the enhanced KRONOS program.

## BACKGROUND

Existing macroscopic flow models fall into three general categories: (a) I/O, (b) simple continuum, and (c) high-order continuum. The models in the first category are rather simplistic in that they do not include space explicitly nor do they take compressibility into account. High-order models, on the other hand, are in principle more realistic as they include the effects of inertia and acceleration of the traffic mass; however, although the existing high-order models look promising, they have not as yet proved truly superior to the simple continuum alternative at least in medium-to-congested flow conditions (*7,8*). For this reason, the current version of KRONOS uses the simple continuum modeling that is based on the conservation equation and an equilibrium speed-density (or flow-density) relationship. However, the program's modeling

Department of Civil and Mineral Engineering, University of Minnesota, 500 Pillsbury Dr., S.E., Minneapolis, Minn. 55455.

methodology and structure are designed to allow use of high-order models if desired. The simple continuum modeling can be described by the partial differential equation

$$\frac{\partial k}{\partial t} + \frac{\partial q}{\partial x} = g(x,t) \qquad \text{with } q = ku = ku_e(k) \tag{1}$$

where

$k$ = density,
$q$ = flow,
$t$ = time,
$x$ = distance, and
$g$ = generation rate.

In order to implement this model, KRONOS uses a finite difference scheme specifically designed to solve one-dimensional, time-dependent, compressible flows containing strong shocks (*12*). With this scheme, the time and space domains are discretized in short increments, $\Delta t$ and $\Delta x$, respectively, such that $\Delta x/\Delta t > u_f$, where $u_f$ is the free-flow speed. Space discretization of a section including the most typical freeway components is shown in Figure 1. The relevant formulas are as follows:

$$k_j(n+1) = \frac{1}{2}[k_{j+1}(n) + k_{j-1}(n)] - \frac{\Delta t}{2\Delta x}[q_{j+1}(n) - q_{j-1}(n)] - \frac{\Delta t}{2}[g_{j+1}(n) + g_{j-1}(n)] \tag{2}$$

$$u_j(n+1) = u_e[k_j(n+1)] \tag{3}$$

$$q_j(n+1) = k_j(n+1) * u_j(n+1) \tag{4}$$

where

$k_j(n)$, $u_j(n)$, $q_j(n)$ = traffic density, speed, and flow, respectively, of Node $j$ at the $n$th time step ($\Delta x$ = 100 ft, $\Delta t$ = 1 sec);
$u_e[k_j(n+1)]$ = equilibrium speed-density relationship, which is location-specific and possibly discontinuous (*13*).

In KRONOS, the flow at the external boundaries (such as upstream and downstream ends of freeway, and the junctions of ramps with the adjacent surface streets) is specified from the arrival and departure pattern provided from input, whereas the flow at the internal boundaries (such as the metering stop-line and the beginning or ending node of deceleration and acceleration lanes, respectively) is determined from either the metering rates or other physical considerations.

In the following sections, the modeling methodology of the enhanced KRONOS is presented along with a description of the program, its capabilities, hardware and software requirements, testing and field validation results, and plans for future improvements.

## MODELING METHODOLOGY OF THE ENHANCED KRONOS

The enhancements that have been made to the KRONOS simulation model since its introduction have been extensive and performed on an ongoing basis. So far, they include improving the treatment of internal boundaries and adding a spillback mechanism for the flow under capacity restraints, such as lane blockage and capacity reduction at the downstream off-ramp caused by construction or arterial traffic con-

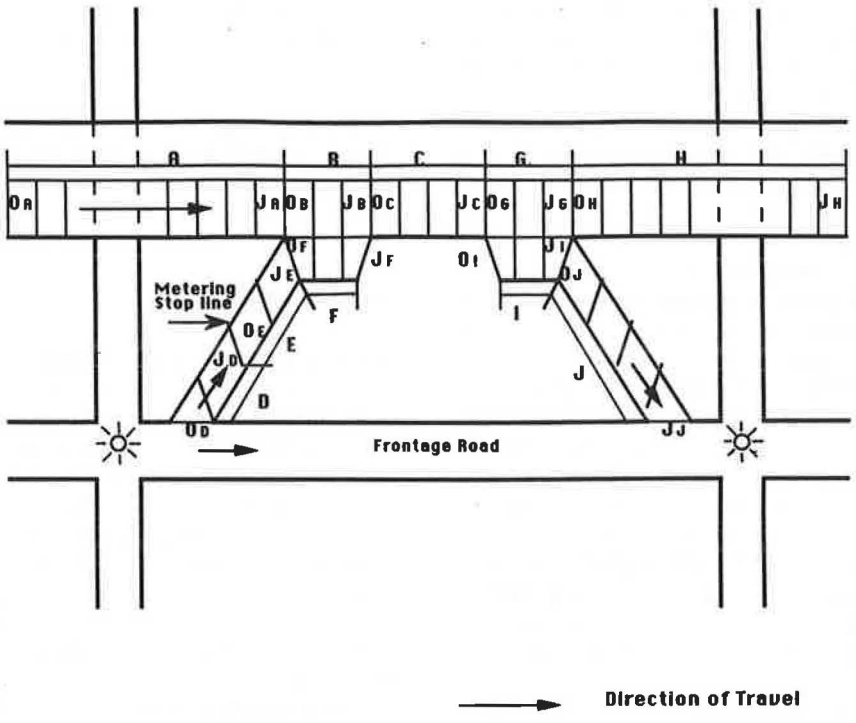


**FIGURE 1 Space discretization of a typical freeway section.**

ditions. In what follows, the basic modeling elements of the aforementioned enhancements are presented to illustrate the basic approach and allow the reader to assess the differences over the earlier modeling. The detailed KRONOS modeling and step-by-step algorithms can be found elsewhere (*10,14*); once again it is stressed that this section contains only the recent modeling improvements in KRONOS, which are summarized in the following sections.

### Links *A*, *D*, *E*, *H*, and *J* (Figure 1)

1. Referring to Figure 1, these links are characterized by the absence of flow generation (dissipation). Calculations for the density of internal Nodes 1 to $J_{M-1}$, where $M = A, D, E, H$, or $J$, follow:

$$k_j(n+1) = \frac{1}{2}[k_{j+1}(n) + k_{j-1}(n)] - \frac{\Delta t}{2\Delta x}[q_{j+1}(n) - q_{j-1}(n)] \quad (5)$$

Speed and flow are calculated by using Equations 3 and 4, respectively.

2. Nodes $O_A$ and $O_D$ in Links $A$ and $D$ are external boundaries, so $q_{OA}(n+1)$ and $q_{OD}(n+1)$ are specified from the input demand patterns.

3. At the ending nodes in Link $H$ and $J$, $q_{JH}(n+1)$ and $q_{JJ}(n+1)$ are specified from the downstream departure rates that can be either restricted with the specified input information or unrestricted. In case of unrestricted departure rates, $q_{JH}(n+1) = q_{JH-1}(n)$, and $q_{JJ}(n+1) = q_{JJ-1}(n)$. When there are capacity restrictions at the ending nodes, $q_{(JH \text{ or } J)}(n+1) = q_{\text{cap, H or J}}(n)$, where $q_{\text{cap, H or J}}(n)$ is the restricted capacity at the last node of Link $H$ or $J$.

4. Nodes $J_D$ and $O_E$ in Links $D$ and $E$ represent the stop line. If the freeway entering demand, $q_{JD-1}(n+1)$, is less than the metering rate, node $J_D$ is not treated as an internal boundary, and thus, the density, speed, and flow at each node in Links $D$ and $E$ are calculated by using Equations 2 to 4. If $q_{JD-1}(n+1)$ is greater than the metering rate, then $q_{JD}(n+1) = q_{OE}(n+1)$ is the metering rate.

5. Following the definition of $q$, the densities of all the internal boundaries can be calculated from the equilibrium $q$-$k$ relationship using the flow rates determined earlier.

6. Density, speed, and flow at the connecting Nodes $J_A$ and $J_E$ are calculated from Equations 2 to 4, respectively. Further, the ending and beginning nodes in consecutive links coincide, that is, $J_A$ in Link $A$ coincides with $O_B$ in Link $B$, $J_E$ with $O_F$ in Link $F$.

### Link F

1. This link represents the acceleration lane and therefore has dissipation terms. Density is calculated from

$$k_j(n+1) = \frac{1}{2}[k_{j+1}(n) + k_{j-1}(n)] - \frac{\Delta t}{2\Delta x}[q_{j+1}(n) - q_{j-1}(n)] - \frac{\Delta t}{2}[g_{j+1}(n) + g_{j-1}(n)] \quad (6)$$

where $g_j(n)$ is the dissipation term calculated from the merging flow in acceleration lane (Link $F$) and the flow in the freeway proper (Link $B$) according to

$$g_{j,F}(n) = \frac{q_{j-1,F}(n-1)}{\Delta x} \frac{[k_{\text{jam}} - k_{j,B}(n-1)]}{\sum_{i=j}^{J}[k_{\text{jam}} - k_{i,B}(n-1)]} \quad (7)$$

where $k_{\text{jam}} - k_{JB}(n-1)$ represents the available storage space at Node $j$ of Link $B$ at the $n$th time step and $k_{\text{jam}}$ is the maximum density. Because the dissipation and generation rates cannot be measured directly for each $\Delta x$, they are calculated by considering the remaining storage space on the freeway merging area as well as the flows in the ramp and freeway.

2. At the beginning node, $q_{OF}(n) = q_{JE}(n)$, $k_{OF}(n) = k_{JE}(n)$; whereas the flow rates at the ending Node $J_F$ are determined by the traffic conditions of the adjacent freeway proper, that is, the Node $J_B$. If the Node $J_B$ is not congested, then $k_{JF}(n+1) = k_{JB}(n)$; otherwise $k_{JF}(n+1) = k_{JF-1}(n)$.

3. With these dissipation rates and boundary conditions, density, speed, and flow at each internal node of Link $F$ can be calculated by using Equation 6.

### Link *B*

Link $B$ represents the freeway merging area. Density is calculated from

$$k_j(n+1) = \frac{1}{2}[k_{j+1}(n) + k_{j-1}(n)] - \frac{\Delta t}{2\Delta x}[q_{j+1}(n) - q_{j-1}(n)] + \frac{\Delta t}{2}[g_{j+1}(n) + g_{j-1}(n)] \quad (8)$$

where $g_j(n)$ is given by Equation 7, but its sign is altered, i.e., $g_{j,F}(n) = -g_{j,B}(n)$. At the beginning and ending nodes, $q_{OB}(n) = q_{JA}(n)$ and $k_{OB}(n) = k_{JA}(n)$, $q_{JB+1}(n) = q_{OC}(n)$ and $k_{JB+1}(n) = k_{OC}(n)$, respectively.

### Link *I*

This link represents the deceleration lane. All the exiting demand is assumed to diverge at the first segment of Link $I$, i.e., at Node $O_I$. The boundary condition of the beginning Node $O_I$ is defined as follows:

$$q_{OI}(n+1) = \min[q_{\text{exit}}(n), q_{\text{poss}}(n)] \quad (9)$$

where

$q_{\text{exit}}(n)$ = exiting demand given by the input data, and
$q_{\text{poss}}(n)$ = possible exit flow rate, given by

$$q_{\text{poss}}(n) = [k_{\text{jam}} - k_{OI}(n)] * \Delta x * 3{,}600/(5{,}280 * \Delta t)$$

where $\Delta x = 100$ ft and $\Delta t = 1$ sec.

With these values of $q_{OI}$ and the corresponding values of $k_{OI}$, calculated from either uncongested or congested region

of the $q$-$k$ curve depending on the downstream condition of Link $I$, Equations 2 to 4 can be applied to calculate the density, speed, and flow at each node of Link $I$.

### Link C

When the capacity at the end of the exit ramp ($J_J$) is restricted, congestion on the off-ramp may spill back onto the freeway (Link $C$); in such case, the through capacity of Link $C$ is reduced. The calculation of the density, speed, and flow values of Link $C$ starts with the determination of any remaining exit demand on this link according to the following steps:

1. Determine the cumulative exiting demand at the Node $J_C$ as follows:

$$R_{JC}(n+1) = R_{JC}(n) + q_{\text{exit}}(n+1) * \Delta t/3{,}600 - q_{OI}(n+1) * \Delta t/3{,}600 \quad (10)$$

where $R_{JC}(n)$ is the cumulative exiting demand remaining on the main line (vph).

If $R_{JC}(n) = 0$, then the Node $J_C$ is not treated as an internal boundary, and Equations 2 to 4 are used for the calculation of $k$, $u$, and $q$ at each internal node of Link $C$.

2. If $R_{JC}(n) > 0$, then the Node $J_C$ is treated as an internal boundary and the through demand and through capacity are calculated as follows:

$$\text{TD}_{JC}(n) = k_{JC-1}(n) * u_{JC-1}(n) * \text{LN}_C \quad (11)$$

$$\text{TC}_{JC}(n) = \text{CAP}_{JC}(n) * (\text{LN}_C - 1)/\text{LN}_C + q_{OI}(n) \quad (12)$$

where

$\text{TD}_{JC}(n)$ = through demand,
$\text{TC}_{JC}(n)$ = through capacity,
$\text{LN}_C$ = number of lanes in Link $C$, and
$\text{CAP}_{JC}(n)$ = capacity of Node $J_C$ given by input data.

3. The boundary conditions of Node $J_C$ are determined as follows: if $\text{TD}_{JC}(n) < \text{TC}_{JC}(n)$, then set

$$q_{JC}(n+1) = \text{TD}_{JC}(n)$$

and calculate the corresponding $k_{JC}(n+1)$ from the uncongested region of the $q$-$k$ curve; otherwise, set

$$q_{JC}(n+1) = \text{TC}_{JC}(n)$$

and calculate $k_{JC}(n+1)$ from the congested region of the $q$-$k$ curve. Finally, using Equations 2 to 4, $k$, $u$, and $q$ at each internal node of the Link $C$ can be calculated with the previous boundary conditions. At the beginning node,

$$q_{OC}(n) = q_{JB}(n)$$

and

$$k_{OC}(n) = k_{JB}(n)$$

### Link G

The beginning node of Link $G$ is treated as an internal boundary whose conditions are determined as follows:

$$q_{OG}(n+1) = q_{JC-1}(n) - q_{OI}(n+1) \quad (13)$$

where $q_{OI}(n+1)$ is given by Equation 9. If Node $O_G$ is uncongested at the previous time step, i.e., $k_{OG}(n) < k_{\text{cr}}$, where $k_{\text{cr}}$ is the density at the capacity flow, then $k_{OG}(n+1)$ is calculated from the uncongested region of the $q$-$k$ relationship using $q_{OG}(n+1)$; otherwise, from the congested region. At the ending node $J_G$,

$$q_{JG}(n+1) = q_{OH}(n+1) \quad (14)$$

$$k_{JG}(n+1) = k_{OH}(n+1) \quad (15)$$

Finally, Equations 2 to 4 are used to calculate the $k$, $u$, and $q$ values at each internal node of Link $G$.

### Treatment of Lane Blockage Caused by Incidents

Figure 2 shows a discretized freeway section with part of its width closed because of an incident. When the reduced capacity of the incident area (Link $B$) is less than the through demand, congestion develops and propagates upstream. In the enhanced KRONOS program, Nodes $J_A$ and $J_B$ are treated as internal boundaries whose conditions are determined as follows:

1. If the through demand, $q_{JA-1}(n)$, is greater than $\text{CAP}_B$ = the capacity of the incident area, then

For Link A, set

$$q_{JA}(n+1) = \text{CAP}_B/\text{LN}_B \quad (16)$$

and calculate the corresponding $k_{JA}(n+1)$ from the congested region of the $q$-$k$ curve.

For Link B,

$$q_{OB}(n+1) = \text{CAP}_B/\text{LN}_B \quad (17)$$

set

$$k_{OB}(n+1) = k_{\text{cr}} \quad (18)$$

If $q_{JA-1}(n) < \text{CAP}_B$, then $q_{JA}(n+1) = q_{OB}(n+1) =$

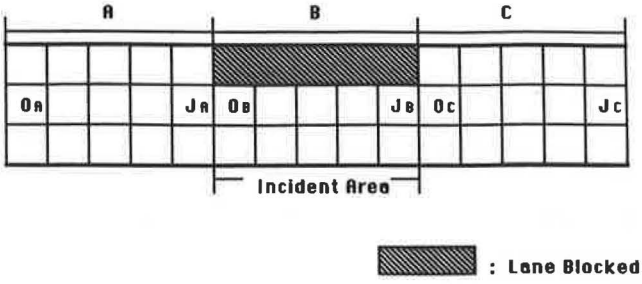


**FIGURE 2 Space discretization of an incident area.**

$q_{JA-1}(n)/\mathrm{LN}_B$, and the corresponding $k_{JA}(n + 1)$ and $k_{OB}(n + 1)$ can be calculated from the uncongested region of the $q$-$k$ curve.

2. At the Node $J_B(O_C)$, the boundary flows are set as follows:

$$q_{JB}(n + 1) = q_{OC+1}(n)/\mathrm{LN}_B \quad (19)$$

$$q_{OC}(n + 1) = q_{OC-1}(n)/\mathrm{LN}_C \quad (20)$$

The corresponding $K_{JB}(n + 1)$ and $k_{OC}(n + 1)$ are calculated from either the uncongested or congested region of the $q$-$k$ relationship, depending on the traffic condition of the downstream Link $C$.

With these boundary conditions, and by using Equations 2 to 4, the density, speed, and flow at each internal node of Links $A$, $B$, and $C$ in Figure 2 can be calculated. The Nodes $O_A$ and $J_C$ can be considered either as external boundaries whose conditions are specified from the input data or as internal nodes when there exist other segments combined with the incident area.

The modeling presented allows simultaneous treatment of the freeway and its ramps in an integrated fashion, where the dynamic interaction between ramps and freeway is explicitly considered through the dissipation-generation terms in the state equations. The numerical scheme adopted in KRONOS provides a stable difference approximation of first-order accuracy with respect to $\Delta t$ (*13*). Further, the internal boundary treatment developed in this study significantly improves flow conservation as well as realistic representation of queue propagation and dissipation through time. In this formulation, there are no restrictions with respect to arrival and departure patterns or the equilibrium $u$-$k$ relationship. Thus, the former could assume any pattern including stochastic ones, and the latter could even be discontinuous.

From $q$, $k$, and $u$, other measures of effectiveness such as total travel, total travel time, delay, energy consumption, and pollution level can be derived. These details, along with the step-by-step algorithms to treat special geometric types such as merging and diverging of two freeways and weaving sections have been provided by Georgadakos et al. (*10*) and Kwon et al. (*14*).

## PROGRAM SUMMARY

The current KRONOS program (Version VI) uses the previously summarized modeling for dynamically calculating speed, flow, and density on each node and segment $\Delta x$ (100 ft). The simulated results of these basic flow parameters are stored in a spreadsheet-formatted output file and the measures of effectiveness (MOE) such as total travel, total travel time, delay, and the duration and extension of congestion (including queue length and size) are derived. These MOE values are summarized by zone (defined as a section between ramps or a merging, diverging and weaving area), as well as by ramp, and presented on the monitor screen. Two- and three-dimensional plots of $k$, $u$, and $q$ are also produced for showing the evolution of these basic variables in space and time and, therefore, visualizing the propagation and dissipation of shock waves and congestion on both the freeway and its ramps. The spreadsheet file containing the detailed simulation results can be accessed by other data management and analysis software such as Lotus 1–2–3, and, thus, much more flexible analysis of the simulation results is possible. For a faster and easier presentation of the propagation of disturbances along the freeway as well as a quick review of its operation (after changes), the discretized form of the freeway is presented on the screen and the density variation of each segment is plotted continuously through time with different colors (from black to red) according to its level.

This output module operation, as well as the input data preparation, is performed interactively in a single-screen environment with on-line help, which minimizes the reference to the manual. For instance, the geometrics are entered by selecting the configuration of each segment from the available alternatives presented on the screen. Figures 3 and 4 show a total of 24 segment types available in the current version of KRONOS as well as an example data input screen. Following definition of the geometrics of each segment, the entire freeway can be plotted for verification. The other input requirements include the freeway and ramp demand patterns in 1- to 15-min time increments (called "time slices"), traffic composition, and departure patterns at exit points, that is, off-ramps and downstream ends of the freeway. Arrival and departure patterns are also plotted for verification and can be as complex as desired. The program allows use of user-specified speed-density models that are entered interactively. The changes to input already entered can be made at any stage during the data entry.

Currently the program can simulate a one-directional freeway section up to six lanes wide and approximately 10 mi long. The section can contain up to 20 entrance and 20 exit ramps, and auxiliary lanes between ramps are permitted. Following is a list of the program's output features:

1. A summary of the MOE indicators for each time slice, including
   a. Total travel, total travel time, and delay;
   b. Total arrivals and departures;
   c. Queue size and length on each ramp; and
   d. Energy consumption and pollution level;
2. Two- and three-dimensional plots of speed, flow, and density as functions of distance or time, or both;
3. Color graphics display of the density variation in the discretized freeway through time;
4. Spreadsheet-type files for flow, speed, and density for further analysis; and
5. Hard copies of two-dimensional plots, including freeway geometrics.

In its present form, the program requires an IBM Personal Computer (PC) (PC/XT, PC/AT, or PS/2) or fully compatible computer with a minimum of 640-kB RAM memory, keyboard, and one 1.2- or 1.44-MB floppy disk drive or a hard disk. It also requires an enhanced color graphics adaptor, a color monitor, and an 80-column (minimum) dot matrix printer with graphics capabilities. The only software required is PC–DOS or MS–DOS operating system, Version 3.0 or later. Simulation time can be substantially reduced if an IBM PC 8087/80287/80387 math coprocessor is added to the system. With an 80386 computer equipped with a 80387 math copro-

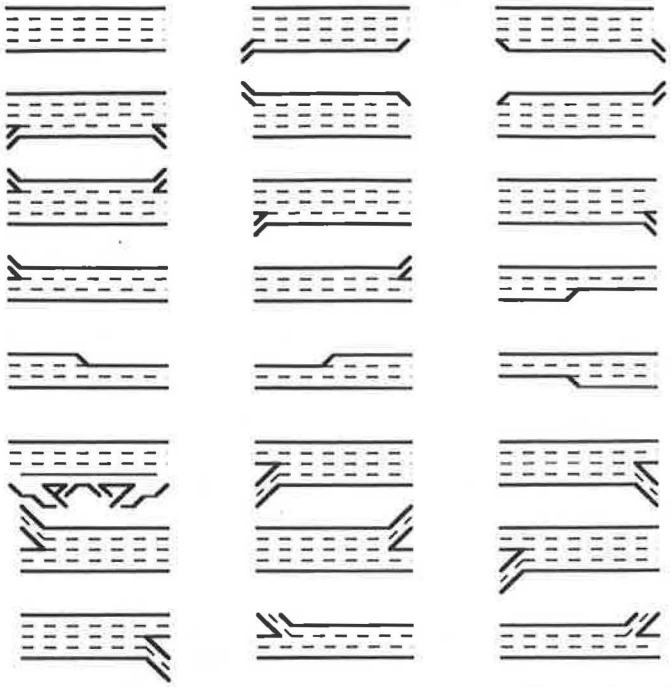

**FIGURE 3 Freeway segment types for synthesizing the geometry of the section to be simulated.**

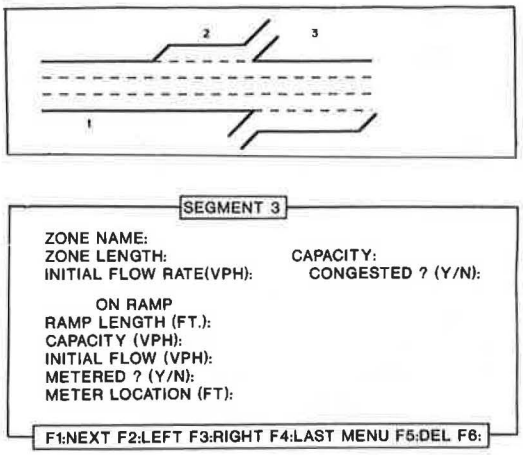


**FIGURE 4 Sample input screen.**

cessor, the program requires approximately 12 min of execution time to simulate a 6-mi freeway section with three lanes for a 1-hr time period.

## PRELIMINARY TESTING

Testing of the modeling was done first by implementing the models to hypothetical situations on an individual basis, that is, by including only one of the merging, diverging, weaving, or other sections at a time rather than a combination of these components. All the 24 potential freeway components (shown in Figure 3) incorporated in the KRONOS-VI program were tested. To illustrate the nature of this testing, which is both intuitive and quantitative, the test results of the spillback mechanism in the diverging area where the off-ramp is closed for 5 min are presented in this section. The detailed test results of other components were provided by Kwon et al. (*14*). Figure 5 shows the geometrics and demand-capacity variation of a hypothetical diverging area, where the upstream demand of the main line and the exiting demand are kept constant at 4,800 and 900 vph, respectively, for 20 min, while the capacity of the downstream off-ramp is reduced from 1,500 to 0 vph for the second 5-min time interval. The simulation results of this hypothetical case are indicated in Figure 6, which shows the density trajectory of the freeway main line at every 3-min time interval. As illustrated in these figures, the model realistically represents the queue build-up process after the ramp is closed as well as the dissipation when the capacity is restored.

Following testing of the model components, several longer freeway sections were tested using the real freeways in Minneapolis, Minnesota. For these sections, only volume data were available from the existing loop detectors. Figure 7 shows the test sections considered. The detailed test results of this preliminary testing were provided by Kwon et al. (*14*); briefly, the volume estimation error, defined as

$$\frac{\sum \left| \begin{matrix} (\text{observed volume} - \\ \text{estimated volume})/\text{observed volume} \end{matrix} \right|}{\text{number of observations}} * 100 \text{ (percent)}$$

ranged from 3 to 8 percent for all short segment types shown in Figure 7. Because of the lack of speed data, a simple $u$-$k$ relationship estimated from the occupancy information was used in this testing.

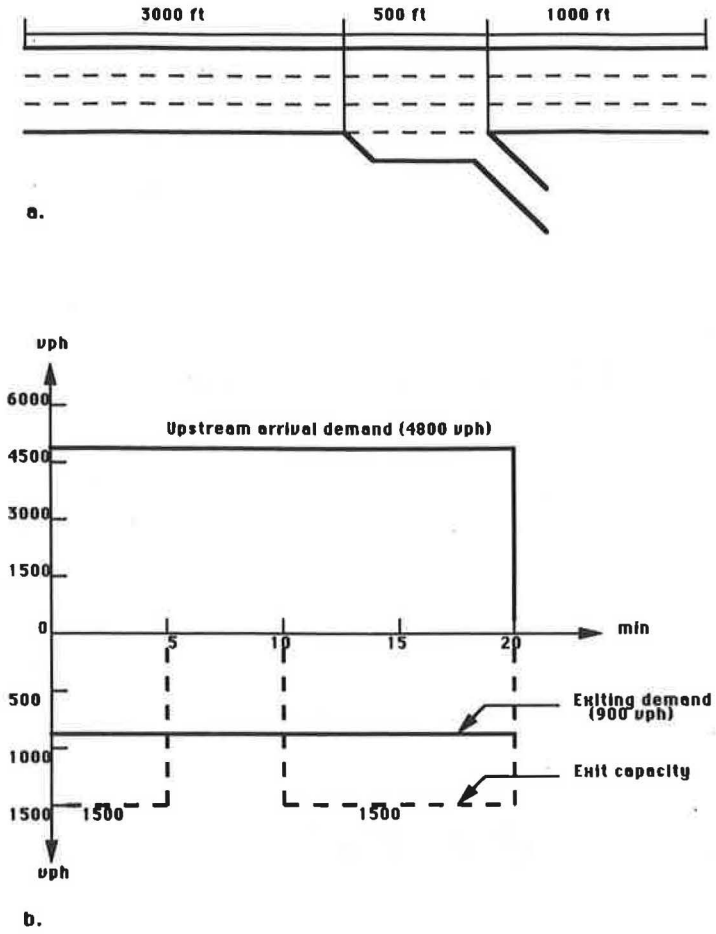


**FIGURE 5 Geometrics and demand pattern of an example diverging area: (a) geometrics, and (b) demand position.**

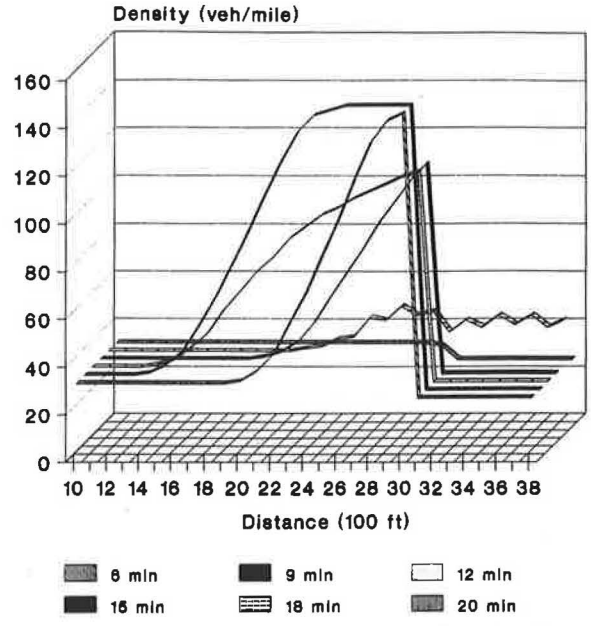


**FIGURE 6 Density trajectory of the example diverging area.**

## FIELD VALIDATION

Although the preliminary test results indicate satisfactory model performance with reasonable accuracy for individual segments, robustness and reliability were not ensured because of the lack of speed data and volume information from all segments. To address this problem, field data collection was recently performed for future validation through a research project funded by the Minnesota Department of Transportation. An 8-mi section of the I-35W freeway was selected as the test site. This section, connecting the Minneapolis downtown to the southern suburban areas, contained 21 entrance-exit ramps as well as a variety of geometric types, such as merging, diverging, weaving, lane addition or deletion at ramps, and so forth. Figures 8 and 9 show schematically both directions of the test freeway section and the data collection sites, which coincided with the locations of in-place loop detectors. Although the loop detectors provided volume and occupancy information, accurate speed information was not directly available from the current Minneapolis detection system. In this study, the speed data were collected manually using stop watches, whereas the volume data were obtained from loop detectors, with the cooperation of the Traffic Management

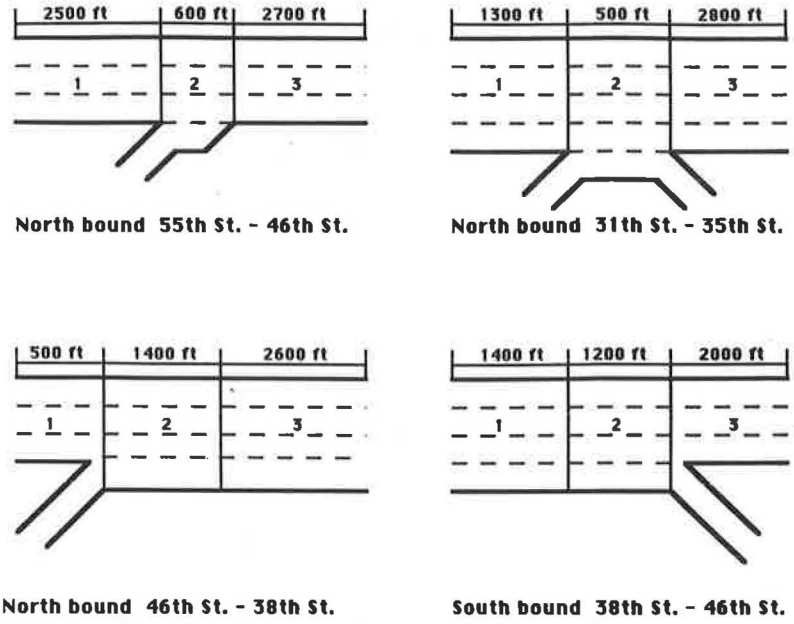


FIGURE 7 Layout of the test sites at I-35W used in the preliminary testing.

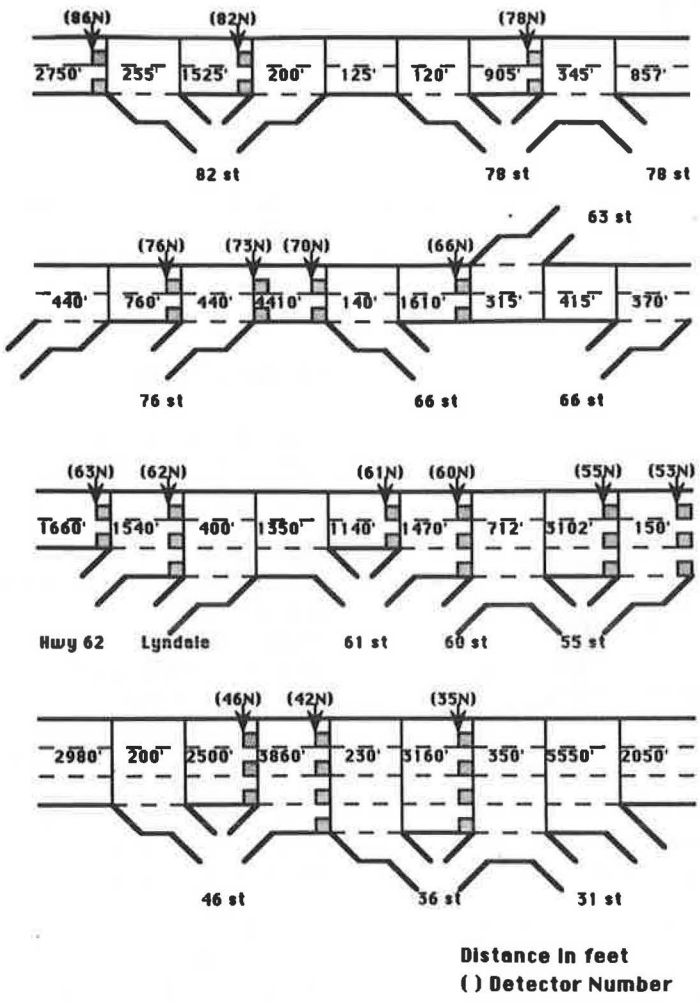


FIGURE 8 Geometrics of the test section (I-35W, Northbound).

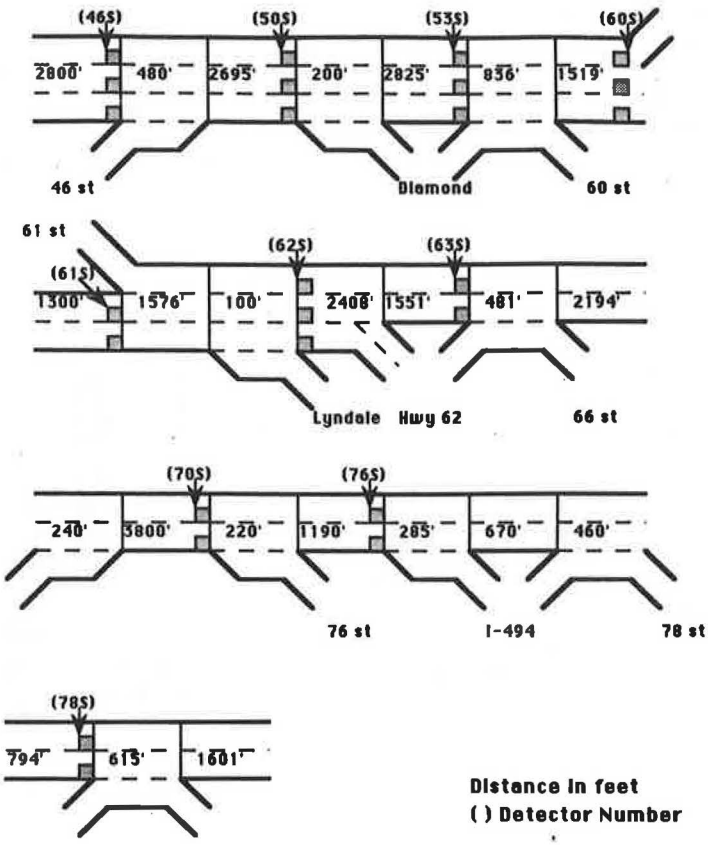


**FIGURE 9 Geometrics of the test section (I-35W, Southbound).**

Center of the Minnesota Department of Transportation. For those sites where the loop detectors were not functioning properly, video recordings or tube detectors were used. Approximately 70 persons were involved to cover 35 collection sites for 6 days during the morning and afternoon peak periods in November 1989.

The data collected from each site include

1. 5-min travel time measurements of vehicles passing between two observation posts for each lane,
2. 5-min volume-occupancy passing the observation posts on the main line (from loop detectors), and
3. 5-min freeway merging-exiting volume from the entrance ramps and to the exit ramps (from either loop or tube detectors).

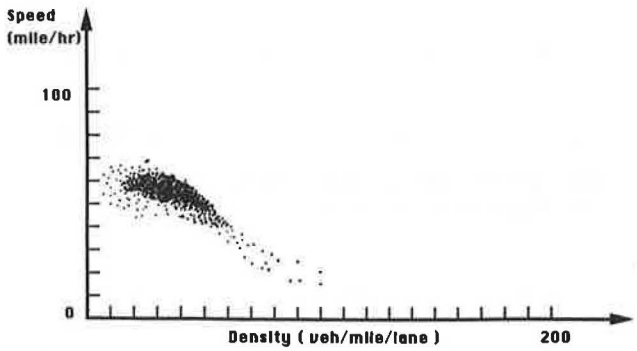


**FIGURE 10 Speed-density relationship derived from the morning measurements.**

Although the morning periods do not include any severe congested situation, snow and heavy congestion occurred in all three afternoons when the data were collected. Approximately 6,500 data sheets were gathered from the 6-day measurements. Each data sheet contained the sample travel time measurements for each lane for every 5-min interval. The information on each data sheet has been stored in computer files and processed to eliminate measurement errors. Because of detector malfunctions, only 4-day measurements were usable for the testing. The remainder of this section summarizes the test results on the basis of the available data.

First, a speed-density relationship was derived from the collected data. Figure 10 shows the speed-density plots derived from measurements for two peak periods (i.e., November 7 and 9 morning data). From these plots, a representative speed-density ($u$-$k$) relationship was derived by fitting a curve to the data points. This curve was entered numerically to KRONOS. Further, the capacity of each individual segment of the sample freeway section was estimated by using the *Highway Capacity Manual* (*15*) and field observations. Using the real volume data collected from the upstream boundary and entrance-exit ramps as the input demand patterns, the 8-mi sample freeway section was simulated with the current geometric conditions and the new $u$-$k$ curve. The resulting comparisons of volume and speed generally indicated close agreement between simulated and actual data. Results at one

typical location where the actual data were collected are shown in Figures 11 and 12, which indicate that speed estimation error is higher than the error in volume estimation.

In order to evaluate the model performance quantitatively, the following error measurements are calculated:

- Percentage difference (PD: %):

$$100 * (\text{measured} - \text{estimated})_k/\text{measured}_k$$

- Mean percentage difference (MPD: %):

$$\Sigma(100 * (\text{measured} - \text{estimated})_k/\text{measured}_k)/N$$

- Mean absolute error (MAE):

$$\Sigma(\text{measured} - \text{estimated})_k/N$$

where $N$ is the number of measured points.

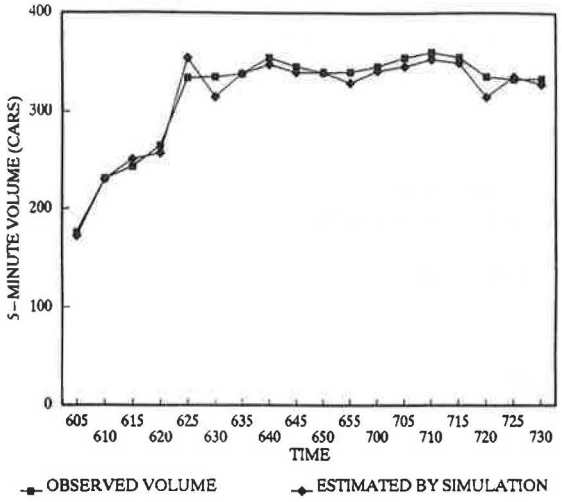


**FIGURE 11 Volume comparison results (Nov. 9, morning period, location: 82N).**

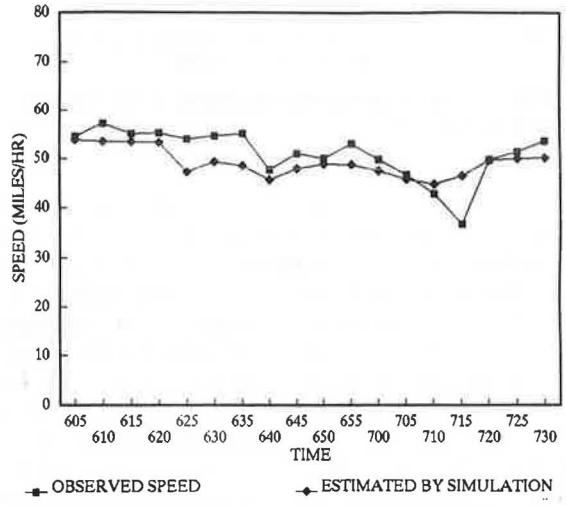


**FIGURE 12 Speed comparison results (Nov. 9, morning period, location: 82N).**

Figures 13–16 show the error (percentage difference) distribution of the 5-min volume-speed estimation results for one morning and one afternoon period, and Tables 1 and 2 present the mean error (MPD and MAE) of each test site for 4 days. As indicated in these figures and tables, the model exhibited satisfactory performance with the morning data set where

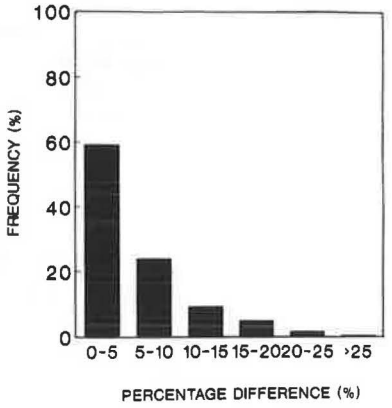


**FIGURE 13 Volume error (PD) distribution during the morning period on Nov. 7.**

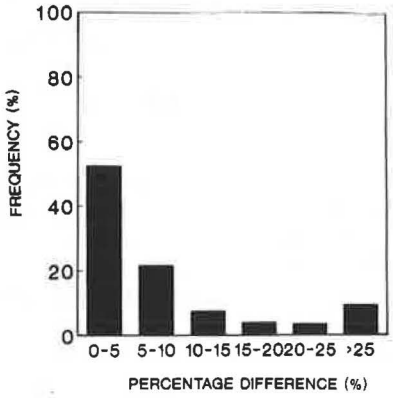


**FIGURE 14 Speed error (PD) distribution during the morning period on Nov. 7.**

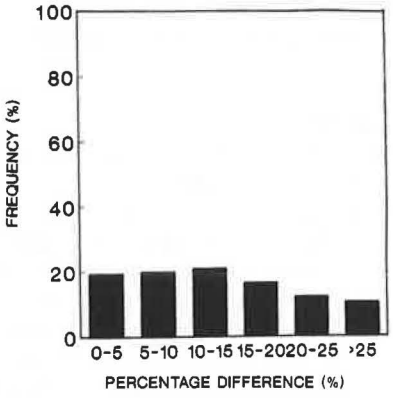


**FIGURE 15 Volume error (PD) distribution during the afternoon period on Nov. 20.**

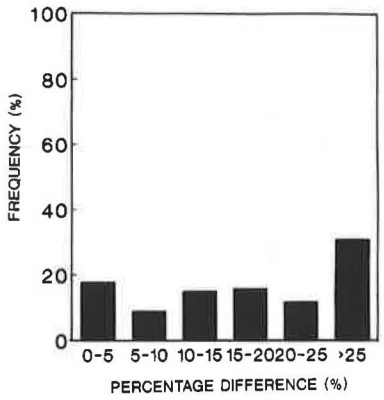


**FIGURE 16 Speed error (PD) distribution during the afternoon period on Nov. 20.**

traffic was relatively uncongested, whereas the estimation error increased in two afternoon peak periods in which traffic was heavily congested because of inclement weather conditions. For example, the comparisons for the November 7, 1989, morning data suggest that, out of 576 data points (16 stations * 36 5-min time intervals) estimated by KRONOS, 92 percent of volume and 82 percent of speed estimation results were within 15 percent of the actual measurements. However, during the afternoon of the November 20 peak period, only 62 percent of volumes and 51 percent of speeds were within 15 percent of the actual measured data. Further, the MPD of volume for two mornings ranges from 0.6 to 15.9 percent, whereas the speed MPD for the same two mornings was between 2.5 and 28.0 percent. For two afternoons, the volume estimation MPD ranges from 7.1 to 27.6 percent and the speed MPD between 2.8 and 31.7 percent.

The higher error in speed estimation indicates the need to use multiple speed-density relationships reflecting weather conditions rather than a single curve throughout. Further, the speed estimation error indicates the need for more effort in calibrating speed-density curves and estimating the capacities. The latter, which is an important issue common to all macroscopic simulation models, is currently being investigated.

Overall, the test results using four peak periods indicate satisfactory performance of the enhanced KRONOS program in light-to-moderate traffic conditions, whereas they indicate further investigation is needed to explain the higher differences during heavy congestion. One possible explanation is the lack of sufficient stable data for deriving the speed-density relationship during such conditions. Clearly, either a new methodology for this procedure or more advanced state equations that do not require use of such relationships have to be developed. Development of such models is currently being considered along with use of high-order continuum models, which, by their nature are truly dynamic as they use a momentum equation.

## CONCLUSIONS AND FUTURE IMPROVEMENTS

The enhanced KRONOS program provides a practical tool for traffic engineers in evaluating various freeway design and

TABLE 1 MEAN ERROR OF THE VOLUME-SPEED ESTIMATION RESULTS (MORNING, 6:00 TO 9:00 a.m.)

| Site | Nov. 7 | | | | Nov. 9 | | | |
|---|---|---|---|---|---|---|---|---|
| | Volume/5-min. | | Speed/5-min. | | Volume/5-min. | | Speed/5-min. | |
| | MPD | MAE* | MPD | MAE** | MPD | MAE | MPD | MAE |
| 86N | 0.7 | 13.6 | 4.6 | 2.3 | 0.6 | 12.3 | 6.9 | 3.8 |
| 82N | 2.5 | 42.6 | 3.3 | 1.9 | 2.3 | 41.9 | 3.8 | 1.9 |
| 78N | 6.6 | 96.6 | 7.8 | 3.7 | 7.8 | 116.8 | 5.6 | 3.2 |
| 76N | 4.0 | 57.3 | 3.7 | 2.5 | 4.4 | 64.6 | 4.8 | 2.5 |
| 73N | 3.5 | 54.3 | N/A | N/A | 5.0 | 79.1 | 6.1 | 3.4 |
| 70N | 3.5 | 53.7 | 3.3 | 1.9 | 4.5 | 72.8 | 4.2 | 2.4 |
| 66N | 4.7 | 65.2 | 2.5 | 1.4 | 5.9 | 82.9 | 4.5 | 2.3 |
| 63N | 14.4 | 196.0 | 5.9 | 2.4 | 15.9 | 221.5 | 16.4 | 5.1 |
| 62N | 8.4 | 133.7 | N/A | N/A | 9.6 | 155.1 | N/A | N/A |
| 61N | 6.9 | 139.8 | 24.2 | 10.5 | 5.9 | 125.3 | 28.0 | 13.3 |
| 60N | 7.1 | 128.0 | 21.8 | 10.5 | 6.9 | 129.7 | 17.3 | 7.3 |
| 55N | 4.6 | 88.2 | 15.4 | 8.2 | 3.9 | 77.4 | 16.5 | 6.8 |
| 53N | 7.1 | 134.2 | 20.5 | 9.3 | 6.5 | 127.1 | 26.1 | 9.8 |
| 46N | 4.9 | 95.7 | 7.9 | 4.3 | 4.1 | 82.1 | 6.1 | 2.4 |
| 42N | 4.8 | 73.8 | 4.4 | 2.6 | 3.4 | 65.0 | 4.0 | 2.4 |
| 35N | 4.2 | 73.3 | 3.8 | 2.1 | 3.6 | 67.8 | 4.9 | 2.7 |

*: veh/hr/lane ** : miles/hr

TABLE 2 MEAN ERROR OF THE VOLUME-SPEED ESTIMATION RESULTS (AFTERNOON, 3:30 TO 6:30 p.m.)

| Site | Nov. 14 | | | | Nov. 20 | | | |
|---|---|---|---|---|---|---|---|---|
| | Volume/5-min. | | Speed/5-min. | | Volume/5-min. | | Speed/5-min. | |
| | MPD | MAE* | MPD | MAE** | MPD | MAE | MPD | MAE |
| 46S | 5.5 | 83.0 | 27.0 | 8.6 | 13.1 | 223.9 | 26.2 | 11.5 |
| 50S | 7.1 | 114.5 | 27.1 | 9.8 | 14.4 | 255.7 | 31.6 | 11.1 |
| 53S | 10.2 | 156.1 | N/A | N/A | 11.5 | 198.1 | 30.3 | 11.5 |
| 60S | 9.2 | 137.3 | 31.4 | 7.1 | 20.8 | 359.2 | 30.8 | 6.0 |
| 61S | 13.9 | 211.8 | 21.8 | 6.6 | 15.7 | 276.7 | 31.7 | 8.3 |
| 62S | 10.4 | 145.2 | 20.7 | 8.7 | 8.2 | 131.8 | 2.8 | 1.3 |
| 63S | 27.6 | 273.6 | 30.2 | 12.4 | 20.0 | 238.5 | 15.6 | 7.1 |
| 70S | 16.1 | 217.8 | 13.6 | 7.3 | 8.4 | 141.3 | 20.0 | 11.2 |
| 76S | 17.1 | 215.4 | 14.6 | 7.5 | 7.9 | 123.3 | 16.4 | 9.4 |
| 78S | 24.1 | 246.2 | N/A | N/A | 17.1 | 224.7 | 7.1 | 3.2 |

*: veh/hr/lane ** : miles/hr

management alternatives, including decisions frequently made in freeway operations, such as ramp metering, lane blockages, construction and maintenance operations, and others. The program, taking advantage of the recent advancements in the microcomputer hardware technology, has the user-friendly menu-driven I/O modules that significantly reduce the time-consuming effort to prepare input and analyze the results. Furthermore, the improvements presented in the earlier sections reduced execution time substantially. In addition, by integrating traffic simulation with advanced data management and analysis software, more flexible and detailed analysis of the simulation results is possible. For example, using the spreadsheet-formatted output file, contour maps of speed, flow, and density that greatly assist the user to follow the generation and propagation of congestion as well as its dissipation can be easily produced. These contour maps are useful for visual (qualitative) assessment of the effects of improvements or incidents, on the freeway. The test results with the field data collected from an 8-mi section of the I-35W freeway indicate promising model performance in estimating volume and speed through time.

Although the data collected in this study provide sufficient information to evaluate the overall performance of the model, more detailed measurements of speed, density, and volume at shorter time and space increments are required to develop accurate models that can be applicable in a real-time environment. Future plans include the collection of such detailed data using the video detection system currently being developed at the University of Minnesota (*16*). A total of 38 video detectors are planned to be installed by 1993 along a 2.5-mi section of the I-394 freeway in Minneapolis, Minnesota (*16*). This section will serve as a live laboratory for collecting and studying traffic characteristics as well as for testing and validating the KRONOS program in a more rigorous fashion by fully analyzing the traffic dynamics in merging, diverging, and weaving areas. Further enhancements to KRONOS currently under consideration also include optimal calibration of multiple speed-density relationships for each section of freeway, high-occupancy-vehicle (HOV) priority treatment, corridor modeling with demand-diversion, estimation of optimal ramp metering rates, and development of high-order continuum models that do not require equilibrium speed-density relationships, and so forth. Finally, an input interface that can automatically extract the necessary input information (geometric and demand) from available data bases will be developed, so that time-consuming manual efforts in preparing the input data can be minimized.

## ACKNOWLEDGMENTS

Funding for this project was provided by the Minnesota Department of Transportation. Jim Aswegan greatly assisted the research team in his role as a project monitor.

## REFERENCES

1. A. D. May. Freeway Simulation Models Revisited. In *Transportation Research Record 1132*, TRB, National Research Council, Washington, D.C., 1988, pp. 94–99.
2. T. Imada and A. D. May. *FREQ8PE: A Freeway Corridor Simulation and Ramp Metering Optimizing Model*. Report UCB-ITS-RR-85-10. University of California, Berkeley, 1985.
3. H. J. Payne. FREFLO: A Macroscopic Simulation Model of Freeway Traffic. In *Transportation Research Record 772*, TRB, National Research Council, Washington, D.C., 1979, pp. 68–75.
4. D. A. Wicks and E. B. Lieberman. *Development and Testing of INTRAS, a Microscopic Freeway Simulation Program*. FHWA-RD-76-75. FHWA, U.S. Department of Transportation, 1980.
5. M. Van Aerde, J. Voss, A. Ugge, and E. R. Case. Managing Traffic Congestion in Combined Freeway and Traffic Signal Networks. *ITE Journal*, Vol. 59, No. 2, Feb. 1989, pp. 36–42.
6. A. K. Rathi and Z. A. Nemeth. FREESIM: A Microscopic Simulation Model of Freeway Lane Closures. In *Transportation Research Record 1091*, TRB, National Research Council, Washington, D.C., 1986, pp. 21–24.
7. P. G. Michalopoulos. A Dynamic Freeway Simulation Program for Personal Computers. In *Transportation Research Record 971*,

TRB, National Research Council, Washington, D.C., 1984, pp. 68–79.
8. P. G. Michalopoulos, D. E. Beskos, and J. K. Lin. Analysis of Interrupted Traffic Flow by Finite Difference Methods. *Transportation Research*, Vol. 18B, 1984, pp. 409–421.
9. P. G. Michalopoulos. Integrated Modelling of Freeway Flow and Application to Microcomputers. *Traffic Engineering Control*, Vol. 27, No. 4, 1986, pp. 198–204.
10. G. Georgadakos, R. Plum, and P. G. Michalopoulos. KRONOS-V: An Interactive Freeway Simulation Program for Personal Computers. Minnesota Department of Transportation, St. Paul, 1988.
11. J. Lin. Numerical Analysis of Traffic Flow in Complex Transportation Networks. Ph.D. dissertation, University of Minnesota, St. Paul, 1985.
12. F. L. Hall and M. A. Gunter. Further Analysis of the Flow-Concentration Relationship. In *Transportation Research Record 1089*. TRB, National Research Council, Washington, D.C., 1988, pp. 1–9.
13. P. D. Lax. Weak Solution of Non-Linear Hyperbolic Equations and Their Numerical Computations. *Communications of Pure and Applied Mathematics*, Vol. 7, 1954, pp. 159–173.
14. E. Kwon, C. F. Lee, J. Kang, et al. Traffic Management Strategies for Freeway Corridors Phase II Extension. Minnesota Department of Transportation, St. Paul, 1990.
15. *Special Report 209: Highway Capacity Manual*. TRB, National Research Council, Washington, D.C., 1985.
16. P. G. Michalopoulos, B. Wolf, and R. Benke. Testing and Field Implementation of the Minnesota Video Detection System. In *Transportation Research Record 1287*, 1990, pp. 176–184.

*Publication of this paper sponsored by Committee on Traffic Flow Theory and Characteristics.*